

# Model-based recovery of histological parameters from multi-spectral images of the colon

Džena Hidović-Rowe and Ela Claridge

School of Computer Science, The University of Birmingham, Birmingham, United Kingdom

## ABSTRACT

Colon cancer alters the macroarchitecture of the colon tissue. Common changes include angiogenesis and the distortion of the tissue collagen matrix. Such changes affect the colon colouration. This paper presents the principles of a novel optical imaging method capable of extracting parameters depicting histological quantities of the colon. The method is based on a computational, physics-based model of light interaction with tissue. The colon structure is represented by three layers: mucosa, submucosa and muscle layer. Optical properties of the layers are defined by molar concentration and absorption coefficients of haemoglobins; the size and density of collagen fibres; the thickness of the layer and the refractive indexes of collagen and the medium. Using the entire histologically plausible ranges for these parameters, a cross-reference is created computationally between the histological quantities and the associated spectra. The output of the model was compared to experimental data acquired *in vivo* from 57 histologically confirmed normal and abnormal tissue samples and histological parameters were extracted. The model produced spectra which match well the measured data, with the corresponding spectral parameters being well within histologically plausible ranges. Parameters extracted for the abnormal spectra showed the increase in blood volume fraction and changes in collagen pattern characteristic of the colon cancer. The spectra extracted from multi-spectral images of ex-vivo colon including adenocarcinoma show the characteristic features associated with normal and abnormal colon tissue. These findings suggest that it should be possible to compute histological quantities for the colon from the multi-spectral images.

**Keywords:** reflectance spectra, colon tissue, physics-based model, Monte Carlo, multispectral imaging

## 1. INTRODUCTION

Development of colon cancer alters the macroarchitecture of the colon tissue. The main changes include an increase in microvascularisation and hence the blood content of the tissue,<sup>1-3</sup> and distortion of its collagen matrix.<sup>4,5</sup> Given that blood and collagen respectively act as strong absorbers and scatterers of light in the visible range of the spectrum, those changes alter the colon colouration. At the early stages of the disease the variations in the colour between normal and abnormal tissue tend to be very subtle, and hence not easily discernible by the human eye. Therefore, a methodology is required which allows the interpretation of the tissue colour in terms of the underlying tissue structure. Standard red, green, blue (RGB) imaging cannot be assumed to be appropriate for colon imaging because spectra from different tissue histologies may produce the same RGB values. This might result in a loss of diagnostically important information. Therefore, a richer spectral data set might be more appropriate for our application. However, full traditional tissue spectroscopy has its own disadvantages, the main one being the fact that the spectroscopy allows extraction of information from a given point only. Analysing larger areas of tissue with this method is quite difficult, and hence potentially suspicious sites can quite easily be missed. An ideal approach would be multispectral imaging, which combines imaging and spectroscopy, and enables the extraction of the whole spectral content at every pixel of the image, so providing the combined advantages of large spatial and spectral resolutions.

In this paper we present the principles of a novel optical imaging method capable of producing histologically informative images showing spatial distribution and relative quantities of blood and collagen in the colon starting

---

Further author information: (Send correspondence to D.H.R.)

D.H.R.: E-mail: D.Hidovic@cs.bham.ac.uk, Telephone: +44 (0)121 414 2884

E.C.: E-mail: E.Claridge@cs.bham.ac.uk, Telephone: +44 (0)121 414 4778

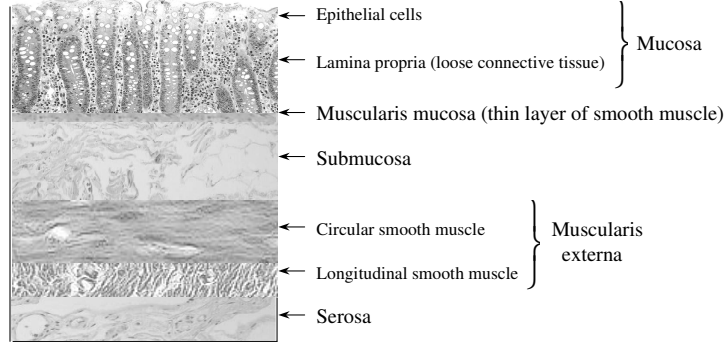


**Figure 1.** Schematic representation of colon architecture.

from multispectral images of the colon. It is believed that the explicit presentation of the relative blood levels and the density of the collagen matrix across the colon should lead to more reliable and possibly earlier diagnosis. The basis of our method is a computational model of colon reflectance. Using the Monte Carlo method of simulating light-tissue interactions, the model correlates tissue parameters which describe its optical properties with the spectral composition of the light that can be observed at the tissue surface after penetrating the tissue and interacting with its structure. Our aim was to use this model for the extraction of tissue information starting from its spectra, and subsequently images. Prior to doing so, the model created had to be validated for correctness. That was done by comparing the spectra calculated by the model and the spectra measured on *in vivo* tissue. As will be shown in section 3, the spectra generated by our model match well the spectra of real tissue, suggesting its correctness. We have subsequently used the model to investigate spatial variations in histological parameters in two *ex vivo* samples of an abnormal colon. This is preliminary work, but the initial results show that the spectra derived from multi-spectral images of the sample show behaviour consistent with the model data.

It has to be stressed here that our approach differs from traditional and more common approaches to image analysis which are based on statistical analysis of the image features. Instead of classifying tissues as normal or neoplastic, we are concerned with understanding the causes of the changes in tissue spectra and hence colour, and correlating those changes to the histological alterations of the tissue.

The rest of the paper is organised as follows. Section 2 presents the model of colon reflectance developed in order to interpret multispectral images of colon. Validating the correctness of the model and its results are presented in sections 3. Section 4 is mainly concerned with the image acquisition set-up and post-processing of images in order to extract the spectral content at each pixel. Analysis of the spectra extracted from multispectral images of colon is given in section 5. We finish the paper with conclusions and by giving some insights into our future work.

## 2. MODEL OF COLON REFLECTANCE

We have developed a computational, physics-based model of light interaction with tissue, which predicts reflectance spectra associated with specific instances of colon tissue. Here we give just a brief description of the model which is described in more detail in our previous papers.<sup>6,7</sup>

The colon structure is represented by three layers: mucosa, submucosa and smooth muscle (see figure 1), which interact with the light incident on the surface of the colon. In all colon layers, the strongest absorbers of light are hemoglobin derivatives, while scattering is done mainly due to collagen and subcellular organelles. These components are characterised by different properties and content in colon layer, which as a consequence have different optical properties, and cause different light-tissue interactions.

The first two layers are each represented by a set of parameters which define its optical properties, shown in table 1. The muscle layer is characterised by scattering and absorption coefficients found in the literature. Three

**Table 1.** Model parameters and their corresponding ranges of values as used in simulations.

Tissue layer	Parameter	Range of values
Mucosa	Volume fraction of blood	2%-10%
	Haemoglobin saturation	50 – 75%
	Size of scattering particles	0.1 – 0.74 $\mu m$
	Density of scattering particles	4 – 20%
	Thickness	395 – 603 $\mu m$
Submucosa	Volume fraction of blood	5 – 20%
	Haemoglobin saturation	50 – 75%
	Size of scattering particles	1 – 6 $\mu m$
	Density of scattering particles	25 – 60%
	Thickness	415 – 847 $\mu m$

additional parameters which influence the light scattering in tissue, namely anisotropy factor, refractive index of the medium and refractive index of the scattering particles, are defined for all three layers of the model. For each of the above parameters, a range of plausible values was defined, ensuring that they correspond to real tissue histology (table 1). Some ranges were taken from literature, while some were derived from our experimental studies and through modelling. For detailed description of parameters, and sources of parameter values please see papers.<sup>6,7</sup>

Once the parameters which define interaction of light with the colon tissue and their normal ranges of values are defined, it is possible to create a cross-reference between the histological quantities and the reflectance spectra, and from this a correspondence between the histology and images. In order to do so, model parameters were used to calculate absorption and scattering properties of various tissue layers (see paper<sup>6</sup> for details and extensive discussions about this). The Monte Carlo method<sup>8</sup> of simulating the light propagation in tissue was then used to calculate the tissue reflectance.

Reflectance spectra of the colon tissue was calculated on a discrete set of the 20 wavelengths chosen to best describe the spectra of colon. In particular, we have used the following wavelength set: {450, 480, 506, 514, 522, 540, 548, 560, 564, 568, 574, 580, 586, 594, 610, 620, 630, 640, 676, 700}. Each spectrum was obtained using 200000 photons.

Our analysis of the spectral dependence on the parameters used to describe optics of colon have shown that the main parameters influencing the light tissue interaction in the colon are the parameters characterising the first layer, namely mucosa, as the propagation of light in the colon is mostly constrained to this layer. However, second and third layers could not be ignored as they define the relative magnitude of the colon spectra, and produce small changes in the red end of the spectrum. For that reason, in the rest of the paper, parameters characterising the first layer are varied in their histologically plausible ranges, while those of submucosa and muscle have been assumed as having constant values set to the middle of their relative ranges. The consequence of this assumption is that the parameters will be extracted just for the mucosal tissue. They should still be of diagnostic value, as the early changes of the colon normally happen in this layer.

### 3. VALIDATING THE MODEL

The model of colon reflectance described above was compared to the spectra measured on real tissue in order to validate its correctness. The idea is that the model is correct only if it produces the spectra that can be measured on real colon tissue. This however is just a necessary, but not also a sufficient condition.

Validation was done by comparing the output of the model to experimental data acquired *in vivo* using a fibre optics probe during colonoscopy procedures.<sup>9</sup> The validation data comprised 50 spectra from histologically confirmed non-neoplastic tissue (normal mucosa) and 7 spectra from cancerous tissue. Parameter values extracted from cancerous tissue were compared to the values extracted from normal colon tissue of the same patient.

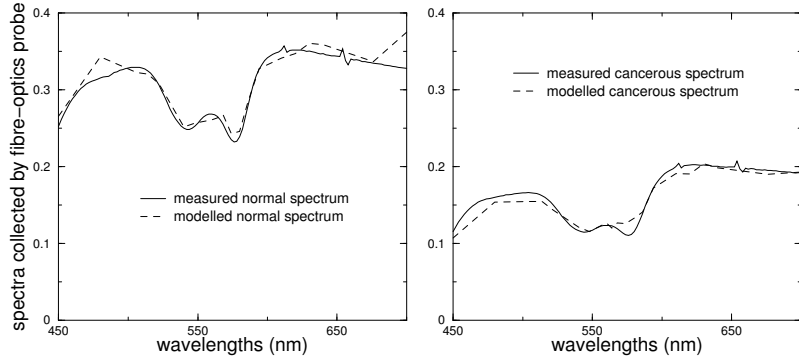


**Figure 2.** a) Typical result of model validation on normal spectra. The modelled spectrum approximates well the measured spectrum. b) The cancerous spectrum from the same patient compared to the output of the extended model. Once again a good match between the measured and the modelled spectrum can be observed.

Extraction of the parameter values from the spectra was implemented as an optimisation procedure. The goal was to find a set of parameter values such that a spectrum generated from the parameters using the Monte Carlo method provides the best match to the measured spectrum. The criterion for the best match is the minimum distance between the two spectra defined as the mean absolute difference between the spectral values at corresponding wavelengths. The optimisation was implemented using an evolutionary strategy<sup>10</sup> which can be briefly summarised as follows. At each step, a set of parameters is chosen and the corresponding spectra calculated. If the distance between the modelled and measured spectra is smaller than some fixed threshold, the procedure is terminated. Otherwise, a new set of parameters is chosen according to a continuous version of the Gray-code neighbourhood distribution<sup>10</sup> and the process repeated.

The model produces spectra which match well the measured data on normal tissue (figure 2.a). The error, measured as the mean absolute distance between the spectra, is  $0.01 \pm 0.0019$ . Parameters extracted from the measured spectra are well within histologically plausible ranges. Comparison of abnormal spectra to the output of the extended model also resulted in good matchings, as shown in figure 2.b. Relative variations of parameters extracted from spectra measured on abnormal tissue, with respect to the spectra of normal tissue of the same patient, were characterised by increased blood content and decreased collagen density (table 2). This is consistent with known histological differences between normal and abnormal colon tissue.

**Table 2.** Parameter values used to generate modelled spectra in figure 2.

Tissue type	Volume fraction of blood	Collagen size	Volume fraction of collagen	Thickness
<b>Normal</b>	3.60%	0.30 $\mu m$	16.4%	483 $\mu m$
<b>Cancer</b>	4.90%	0.25 $\mu m$	7.6%	511 $\mu m$

#### 4. MULTISPECTRAL IMAGING OF THE COLON

Having validated the model on single point spectra, we have carried out a small scale validation using data obtained from multispectral images. Single spectra are normally acquired using a specialised probe placed at a small distance from the colon tissue. In image acquisition using a digital camera the imaging conditions such as distance between the tissue and the sensor, the magnitude and angular distribution of the illuminating light, etc, are more difficult to control than in spectroscopy. In the validation experiment multispectral images of the *ex vivo* colon tissue were acquired, and from those the whole spectral content at each image pixel was extracted. The experiment was carried out on two tissue samples obtained during two surgeries performed at the Queen

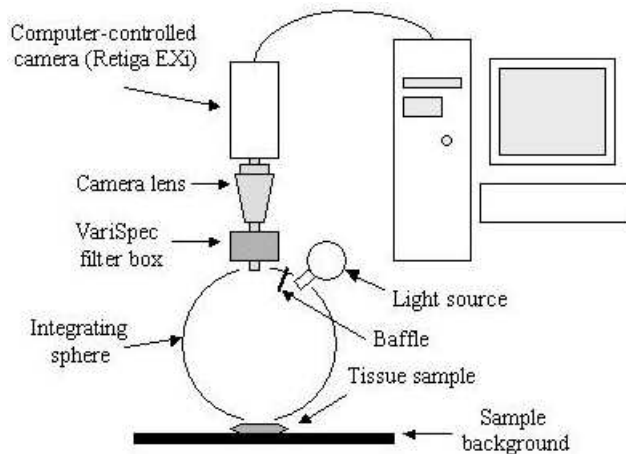


**Figure 3.** Diagram of the imaging setup.

Elizabeth Hospital in Birmingham (UK). For our experiment we have selected apparently normal tissue samples about 20cm and 10cm away from histologically confirmed cancerous tissue, and the cancerous site itself. Images were acquired within one hour of tissue extraction. After extracting the tissue from the body, the colon sample was cut open. Prior to putting the tissue into fixative which slows down the changes in tissue structure that occur in the *ex-vivo* tissue, the sample was pinned down on a black surface, in order to flatten it for imaging. A black surface was chosen so as to avoid any influence of the background on the images of the colon.

#### 4.1. Imaging setup

The system used for acquiring the images consisted of: a Retiga EXi (QImaging, Canada) 12bit monochrome camera, VariSpec (CRI, U.S.A.) liquid crystal tunable filters, and an Integrating Sphere (ProLite, U.K.). The VariSpec filters allow the selection of Gaussian-shaped filters of halfwidth 5-7 nm in the range from 400 to 700 nm (figure 4) by specifying the middle wavelength of the filter. The integrating sphere was used because its light source produces a smooth illumination, especially in the range above 450nm. The total acquisition time was less than 5 seconds.

The VariSpec filters were mounted in front of the camera lens and positioned at the camera aperture of the integrating sphere, while the extracted colon tissue was placed at the opposite aperture of the sphere (a diagram of the setup is shown in figure 3). Light falling on the tissue had a completely randomised direction after passing through the sphere. After interacting with the underlying tissue, light passing through the VariSpec box was filtered, and only the portion with the desired wavelength bands was passed and collected by the camera. In order to reproduce the main spectral characteristics of the exiting light, multiple images of the same tissue sample were acquired at many different wavelengths. In particular, we have acquired images using 33 filters with the following central wavelengths: {460, 465, 470, 475, 480, 485, 490, 495, 500, 506, 514, 522, 540, 548, 560, 564, 568, 574, 580, 586, 594, 610, 615, 620, 625, 630, 635, 640, 645, 655, 676, 685, 700 } (figure 4). Wavelengths below 450 were not considered because quantum efficiency of the camera in that region and intensity of illuminating light were quite poor. In addition, transmission of light by VariSpec filters in the lower half of the blue region is very small. These facts give rise to a very low signal to noise ratio below 450 nm.

#### 4.2. Extraction of spectra

The acquired images were aligned using a computer program which makes use of MATLAB functions for image registration (cpselect, cpcorr, cp2tform and imtransform). An example set of images of the normal colon at wavelengths 455, 540 and 676 respectively is shown in figure 5. A corresponding set of images of cancerous tissue is shown in figure 6. Large circles visible on the images represent the aperture of the sphere, with a diameter of 3 inches. It can be observed that blood vessels and smaller features of the tissue can be seen in the mid green

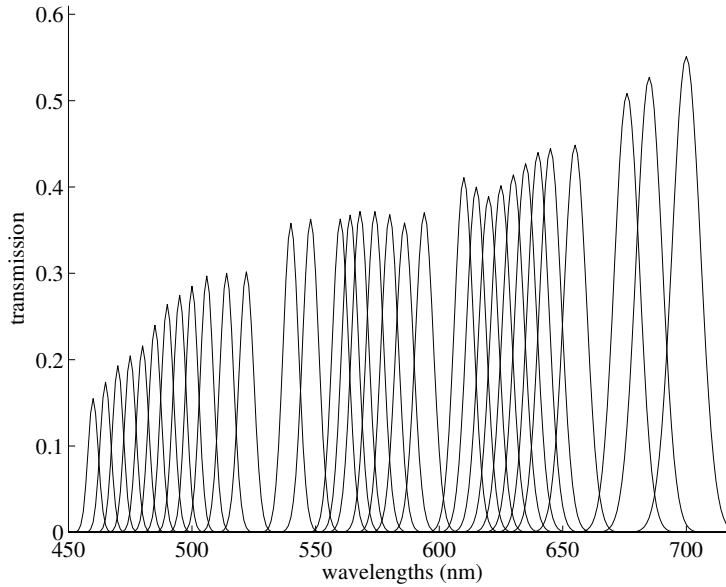


**Figure 4.** VariSpec filters used in imaging.

region (540 nm) where blood absorption is strong. In the blue region (455 nm) the features are less distinct because high blood absorption coefficient causes even small amounts of blood to absorb strongly thus reducing differentiation between high and low blood levels. In deeper red (676 nm) those features seem to disappear because of small absorption of light by hemoglobin derivatives present in the blood.

After alignment, at each pixel point  $(x,y)$ , the image value  $i_\lambda(x,y)$  corresponding to filter centred at wavelength  $\lambda$  is a function of the tissue properties, incident light and the characteristics of the image acquisition system:

$$i_\lambda(x,y) = \int_w R(x,y,w) \cdot I(w) \cdot e(w) \cdot f_\lambda(w) dw \quad (1)$$

where  $R(x,y,w)$  is tissue reflectance at the pixel  $(x,y)$  at the wavelength  $w$ ,  $I(w)$  is intensity of incident light at  $w$ ,  $e(w)$  quantum efficiency of the camera,  $f_\lambda(w)$  spectral response of the filter centered at  $\lambda$ , at the wavelength  $w$ .

The feature of interest is the tissue reflectance,  $R(x,y,w)$ . In order to extract it from the acquired images, filter  $f_\lambda$  was approximated as a single spike at  $\lambda$ , and all pixels in all the images were normalised by the relative magnitude of the illuminant, camera efficiency and filter transmission values. These quantities were available as a function of wavelength from instrument calibration. The resulting reflectance values were adjusted for the exposure time and camera gain used during acquisition.

The analysis was carried out on approximately 30% of the pixels corresponding to the four tissue types: normal colon with discernable blood vessels, normal colon with no blood vessels visible, the cancerous polyp, and the unequivocal area of tissue adjacent to the polyp. In the Results section representative spectra from these four tissue types are presented and discussed.

## 5. RESULTS

The model presented earlier on in this paper had to be slightly modified before it could be use for the analysis of the multispectral images of *ex-vivo* colon tissue. In particular, given that *ex-vivo* tissues have lower blood content

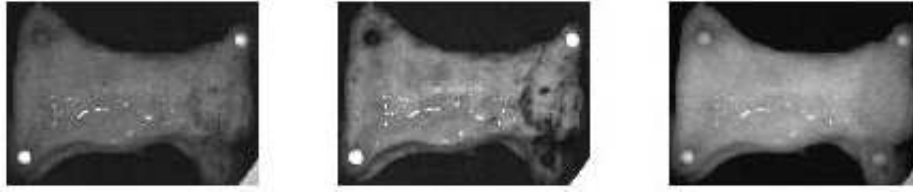


**Figure 5.** Images of normal colon tissue at wavelengths (from left to right) 455, 540 and 676 nm.

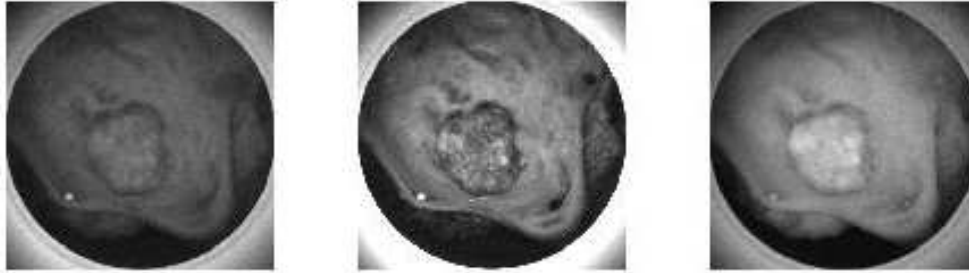


**Figure 6.** Images of cancerous colon tissue at wavelengths (from left to right) 455, 540 and 676 nm.

and that the partial de-hydration of the tissue results in a decrease of layer thickness, the lower boundaries of the ranges corresponding to these two parameters had to be set to a lower value.

Left graph in figure 9 shows the extracted spectra corresponding to normal colon tissue. Before analysing and further discussing the spectra, two observations have to be made here. Firstly, measured spectra shown in figures 2 and 9 have different spectral content. The reason for this is that they were measured using different acquisition geometries. The spectra of *in vivo* tissue were acquired using a contact fibre optics probe. That type of the probe is generally known to be more sensitive to reflectance in blue and green regions of the visible light, while a large proportion of the light in the red region, which travels deeper in the tissue, is not recorded by the probe because it emerges at the tissue surface at distances larger than separation between light delivering and collecting fibres. Our imaging setup, on the other hand, is less sensitive to lower wavelengths. This obviously has to be taken into account when comparing the measured and modelled spectra.

Second note has to be made with respect to the shape of the spectra extracted from multispectral images. Careful observation of measured spectra in figure 9 reveals that its shape seems to be slightly tilted and aligned along virtual axis  $y = ax + b$  ( $a, b > 0$ ). Differences between the model and the measured spectra had characteristics profile similar to our illuminating light. This suggests that a small percentage of the incident light, which bounced off the inside of the sphere without making a contact with the sample, was collected by camera. Therefore, before comparing the spectra, measured spectra were further corrected by subtracting from them a small fraction of the illuminating light.

From figure 9 it can be observed that measured spectra show features characteristic of absorption by haemoglobin derivatives in alpha and beta bands, which implies that tissue samples were not completely deprived of blood. This was true for both normal and cancerous samples (see figure 10). In normal tissue, which is considered to have quite consistent structural and hence optical properties, the spectral composition was also consistent. Except for the differences in the intensity of the remitted light corresponding to the non-evenly illuminated tissue sites, the main differences in the spectral content were associated with the tissue characterised by the presence or absence of immediate sub-surface blood vessels. Those differences were mainly confined to the green part of the spectrum, where blood absorption is strong, so larger blood content implies large light absorption and hence reflectance is smaller. The same spectral behaviour can be observed on the right-hand-side graph in figure 9 showing modelled spectra generated with lower (solid line), and larger (dashed line) blood content.

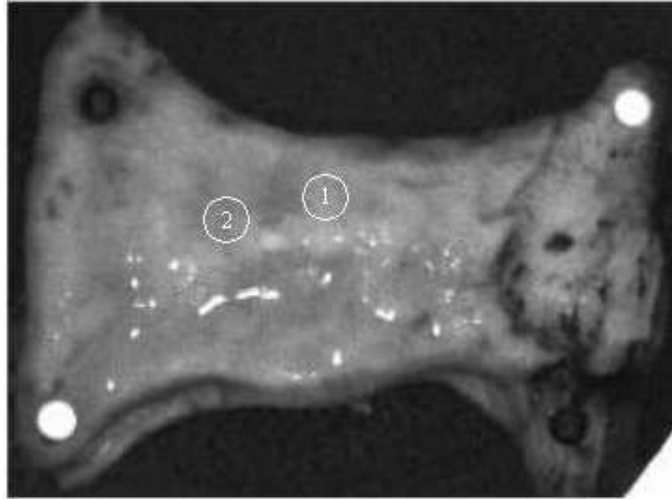


**Figure 7.** Normal colon at 540nm, with marked example area of tissue with no blood vessel (1), and where a vessel is visible (2). Spectra of normal tissue presented in the paper were taken from these sites.

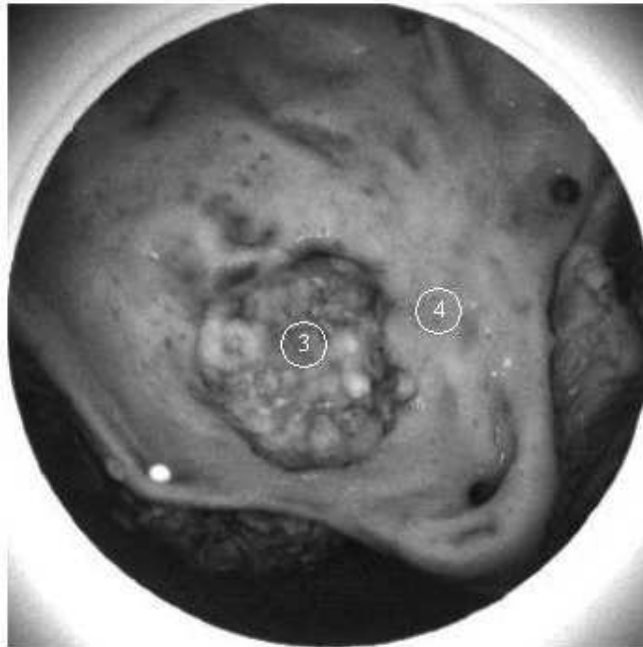


**Figure 8.** Abnormal tissue at 540nm. Marked are area of adenocarcinoma (3) and surrounding tissue (4) from which the spectra shown in the paper was taken.

In the images of the abnormal tissue (figure 6), we can observe two different tissue types. One is a polyp in the middle of the image, distinguishable by its characteristic shape and texture, which was histologically confirmed as an adenocarcinoma. The second is the tissue around the polyp. A comparison of the spectra of cancerous and normal tissue (10 cm away from the cancer) is shown on figure 10. Once again, graph on the left shows measured spectra. The main spectral variations seem to be due to larger blood content of the cancerous polyp (corresponding spectrum is lower in blue and green bands), and larger mucosal thickness (the red end of the spectrum is higher). The spectra are consistent with know histological variations that occur with development

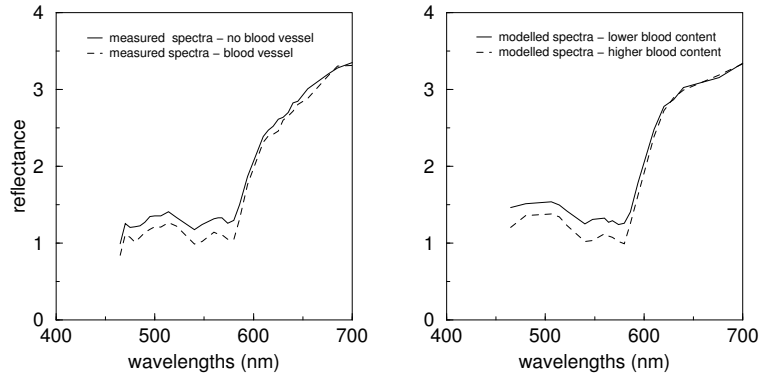


**Figure 9.** Spectra of normal colon tissue. The left graph shows measured spectra: solid line is a spectrum of tissue with no visible blood vessels (marked 1 on figure 7), while dashed line is a spectrum of tissue with visible blood vessels (marked 2 on figure 7). On the right, we see the analogous spectral behaviour on the modelled spectra achieved by increasing blood content.

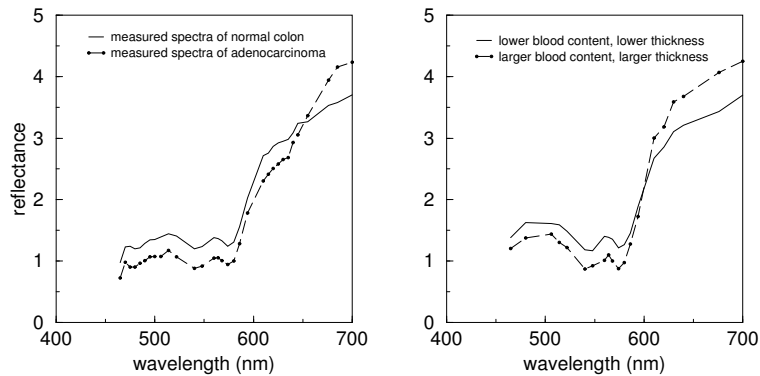


**Figure 10.** Comparison of spectra of normal and cancerous colon tissue. The left graph shows measured spectra: solid line is a spectrum of normal tissue (marked 1 on figure 7), while dashed line is a spectrum of histologically proven adenocarcinoma (marked 3 on figure 8). On the right, analogous spectral differences are visible in the modelled spectra if blood content and thickness are increased (dashed line) with respect to normal tissue (solid line).

of malignancy. Analogous spectral variations were reproduced by our model, and shown on graph on the right of figure 10.

Finally a comparison between spectra of the cancer and the surrounding tissue was made. The proximity of the polyp means that the surrounding tissue may have also undergone structural and cellular changes, not necessarily cancerous, but such that the tissue could not be classified as normal any more. It is, therefore, interesting to see what kind of spectral changes may have been induced. Figure 11 shows that, similarly to cancerous and normal tissue, main spectral variations seem to be due to larger blood content and mucosal thickness of the cancerous polyp. However, difference in blood content is slightly smaller than difference in blood content between cancer and normal tissue, indicating the increase in microvasculature also in the surrounding tissue.

## 6. CONCLUSIONS AND FUTURE WORK

The model correctly predicts the spectra, and thus colours, of colon tissue, indicating that histological quantities can be computed from colours measured by a digital camera. First results carried out on the extended model suggest that it could be used to differentiate between normal and abnormal tissue, which would potentially

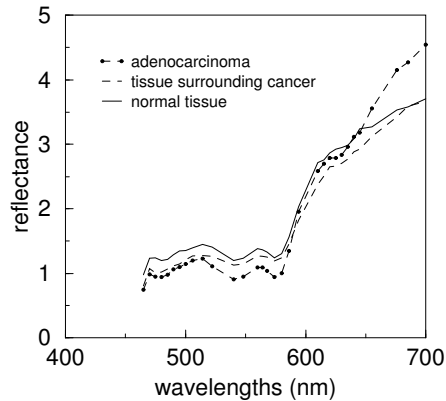


**Figure 11.** Comparison of spectra of all three tissue types: solid line is a spectrum of normal colon tissue (marked 1 on figure 7); dashed line is a spectrum of cancer surrounding tissue (marked 4 on figure 8), while dot-dashed line is a spectrum of histologically proven adenocarcinoma (marked 3 on figure 8).

make it a useful aid in the early detection of colon cancer. Preliminary studies on multispectral images of the colon suggest that they are capable of representing spectral information equivalent to that obtained by point spectrometry. Following these positive results, a larger study is under way. With spectral information available at each pixel, the model of colon reflectance described in section 2 could be used for analysing spatial variations of the tissue components.

Work is currently being undertaken in order to optimise the choice of filters to use in the acquisition of multi-spectral images of tissue so as to maximise the efficiency of extraction of histological quantities starting from those images and using the model. Earlier work by our group has shown that under certain conditions it is possible to recover parameter values relatively accurately from a small number of optimally selected spectral bands.<sup>11</sup> Four parameters characterising the mucosa (thickness, blood volume fraction, size, and density of collagen fibrils - see section 2) require four bandpass filters, making the image acquisition with the existing endoscope technology feasible.

The main criterion for selection of the bandpass filters for imaging is minimisation of the error in parameter recovery. There are a number of sources of error inherent in image acquisition and subsequent model-based interpretation of the images:

- error in the image acquisition, characteristic of the acquisition setup
- error in scattering and absorption coefficient
- Monte Carlo error, due to stochastic nature of the method

Once the optimal filters are found, the relationship between the multi-spectral image vectors and the parameters can be derived from the spectral reflectance model described in this paper as follows. By varying the model parameters across the whole range of their plausible values, reflectance spectra corresponding to all normal colon tissues can be generated. By convolving the spectra with the four bandpass filters selected through optimisation, all plausible 4-dimensional image vectors can be computed. In this way the cross-reference between the tissue parameters and the image vectors is established. Provided that the mapping between the parameters and image vectors is unique,<sup>11</sup> parameter values can be derived from the measured four-band image data. Information about the histological parameters characterising the colon can then be represented in a form of grey-scale images (parametric maps) with each pixel showing the magnitude of the respective parameter. This should permit the reconstruction of the structure of colon tissue and its further analysis.

## 7. ACKNOWLEDGEMENTS

Kevin Schomacker (MediSpectra, Inc) is gratefully acknowledged for providing us with *in vivo* spectral reflectances of colon tissue, and Jon Rowe (University of Birmingham) for his help and guidance, especially with optimisation algorithms. We would also like to thank very much Mr Tariq Ismail (University Hospital Birmingham), and Dr Nigel Suggett and Dr Emma Hamilton (University of Birmingham) for their help with endoscopic images of colon, and for providing us with tissue samples.

## REFERENCES

1. S. A. Skinner, G. M. Frydman, and P. E. O'Brien, "Microvascular structure of benign and malignant tumors of the colon in humans," *Digest. Dis. Sci.* **40**, pp. 373–84, 1995.
2. S. A. Skinner and P. E. O'Brien, "The microvascular structure of normal colon in rats and humans," *J. Surg. Res.* **61**, pp. 482–90, 1996.
3. G. C. Zografos, S. Y. Iftikhar, J. Harrison, and D. L. Morris, "Evaluation of blood flow in human rectal tumors using a laser doppler flowmeter," *Eur. J. Surg. Oncol.* **16**, pp. 497–499, 1990.
4. J. Turnay, N. Olmo, J. Gavailanes, and M. Lizarbe, "Collagen metabolism in human colon adenocarcinoma," *Conn. Tiss. Res.* **23**, pp. 251–60, 1989.
5. Y. Furuya and T. Ogata, "Scanning electron microscopic study of the collagen networks of the normal mucosa, hyperplastic polyp, tubular adenoma and adenocarcinoma of the human large intestine," *Tohoku J. Exp. Med.* **169**, pp. 1–19, 1993.
6. D. Hidović-Rowe and E. Claridge, "Modelling and validation of spectral reflectance for the colon." To appear in *Phys. Med. Biol.*
7. D. Hidović-Rowe and E. Claridge, "Model based recovery of histological parameters starting from reflectance spectra of the colon," To appear in *SPIE Proc. of Saratov Fall Meeting 2004*.
8. L. Wang and S. L. Jacques, "Monte Carlo modelling of light transport in multi-layered tissues in standard c," *Univ of Texas, MD Anderson Cancer Center*, 1998.
9. Z. Ge, K. T. Schomacker, and N. S. Nishioka, "Identification of colonic dysplasia and neoplasia by diffuse reflectance spectroscopy and pattern recognition techniques," *Appl. Spectrosc.* **52**, pp. 833–9, 1998.
10. J. E. Rowe and D. Hidović, "An Evolution Strategy using a continuous version of the Gray-code neighbourhood distribution," in *Proc. GECCO 2004*, K. Deb, ed., *Lecture Notes in Computer Science* **3102**, pp. 725–736, Springer-Verlag, 2004.
11. E. Claridge and S. J. Preece, "An inverse method for the recovery of tissue parameters from colour images," in *Inform. Process. Med. Imag.*, C. Taylor and J. A. Noble, eds., **LNCS 2732**, pp. 306–317, Springer, 2003.